

**Memory in nanomagnetic systems: Superparamagnetism versus spin-glass behavior**Malay Bandyopadhyay<sup>1</sup> and Sushanta Dattagupta<sup>1,2,\*</sup><sup>1</sup>*S.N. Bose National Centre for Basic Sciences, JD Block, Sector III, Salt Lake, Kolkata 700098, India*<sup>2</sup>*Jawaharlal Nehru Centre for Advanced Scientific Research, Jakkur, Bangalore 560064, India*

(Received 3 June 2006; revised manuscript received 15 September 2006; published 13 December 2006)

The slow dynamics and concomitant memory (aging) effects seen in nanomagnetic systems are analyzed on the basis of two separate paradigms: superparamagnets and spin glasses. It is argued that in a large class of aging phenomena it suffices to invoke superparamagnetic relaxation of individual single domain particles but with a distribution of their sizes. Cases in which interactions and randomness are important in view of distinctive experimental signatures are also discussed.

DOI: [10.1103/PhysRevB.74.214410](https://doi.org/10.1103/PhysRevB.74.214410)

PACS number(s): 75.75.+a, 75.50.Lk, 75.50.Tt, 75.47.Lx

**I. INTRODUCTION**

The subjects of both superparamagnetism and spin glasses are quite old and well studied.<sup>1-7</sup> Yet they have been rejuvenated in recent years in the context of fascinating memory and aging properties of nanomagnets. These properties, which are believed to be of great practical use, have been recently investigated in a large number of experiments on magnetic nanoparticles.<sup>8-15</sup> The observed slow dynamical behavior has been variously interpreted, based on the paradigm of either superparamagnet or spin glass, sometimes even obscuring the difference between the two distinct physical phenomena. The purpose of this paper is to reexamine some of the data, others' as well as our own, and critically assess the applicability of the physics of either superparamagnets or spin glasses and, occasionally, even a juxtaposition of the two. Our main point is that spin glasses are marked by complexity, arising out of two separate attributes—frustration and disorder. While the manifested properties, such as stretched exponential relaxation and concomitant aging effects, can also occur due to “freezing” of superparamagnetism, especially in a polydisperse sample, the physics of spin glasses is naturally much richer than that of superparamagnets. A discernible experimental signature of superparamagnetism versus spin-glass behavior seems to be the magnitude of the field-cooled (FC) magnetization memory effect that is significantly larger for the interacting glassy systems than the one in noninteracting superparamagnetic particles.<sup>16</sup> Therefore, invoking spin-glass physics in interpreting data on the slow dynamics of nanomagnets can sometimes be like “killing a fly with a sledge hammer,” especially if a simpler interpretation on the basis of superparamagnetism is available. We explore such situations in this paper.

Superparamagnetism was discussed quite early by Frenkel and Dorfman and later by Kittel as a property arising out of single-domain behavior when a bulk ferromagnetic or an antiferromagnetic specimen is reduced to a size below about 50 nm<sup>2</sup>. For such a small particle size the domination of surface to bulk interactions yields a monodomain particle inside which nearly 10<sup>5</sup> magnetic moments are coherently locked together in a given direction, thus yielding a giant or a supermoment. Clearly, for this to happen, the ambient temperature must be much less than the bulk ordering tempera-

ture, so that the integrity of the supermoment is maintained. However, as Néel pointed out, in the context of magnetic properties of rocks in geomagnetism, the direction of the supermoment is not fixed in time.<sup>1</sup> Indeed, because of thermal fluctuations, this direction can undergo rotational relaxations across an energy barrier due to the anisotropy of the single-domain particle, governed by the Néel relaxation time:

$$\tau = \tau_0 \exp\left(\frac{KV}{k_B T}\right). \quad (1)$$

In Eq. (1), the preexponential factor  $\tau_0$  is of the order of 10<sup>-9</sup> sec,  $V$  is the volume of the particle, and  $K$  is the anisotropy energy, the origin of which lies in the details of all the microscopic interactions. For our purpose  $K$  would be treated as a parameter whose typical value is about 10<sup>-1</sup> J/cm<sup>3</sup>. Therefore, at room temperature,  $\tau$  can be as small as 10<sup>-1</sup> sec for a particle of diameter 11.5 nm but can be astoundingly large as 10<sup>9</sup> sec for a particle of diameter just about 15 nm. Thus a slight polydispersity (i.e., a distribution in the volume  $V$ ) can yield a plethora of time scales, giving rise to interesting slow dynamics. For instance, if  $\tau < \tau_E$ , where  $\tau_E$  is a typical measurement time in a given experiment, the supermoment would have undergone many rotations within the “time window” of the experiment, thereby averaging out to zero the net magnetic moment. One then has superparamagnetism. On the other hand, if  $\tau > \tau_E$ , the supermoment hardly has time to rotate within the time window, thus yielding a “frozen-moment” behavior. The consequent nonequilibrium features have led to the phrase “magnetic viscosity,” while depicting the time-dependent freezing of moments.<sup>3,4,17,18</sup> Further, the transition from superparamagnetism to frozen-moment behavior occurs at a temperature, referred to in the literature as the blocking temperature  $T_b$ , defined by

$$\tau_E = \tau_0 \exp\left(\frac{KV}{k_B T_b}\right). \quad (2)$$

When the measurement temperature  $T$  is less than  $T_b$  the magnetic particles are blocked, whereas in the other extreme they display facile response to applied fields. Therefore, we emphasize that even within a single particle picture, *sans* any form of interparticle interactions, such as in a dilute nanomagnetic specimen, one can obtain apparently intriguing ef-

fects such as “stretched exponential” relaxation simply because of size distributions. The latter will be shown to be responsible for much of the data on slow relaxations in nanomagnets.

Turning now to spin glasses, historically the phenomenon was first observed in dilute alloys such as  $Au_{1-x}Fe_x$  (or  $Cu_{1-x}Mn_x$ ) in which magnetic impurities Fe (or Mn) in very low concentrations were “quenched in” from a solid solution with a host metallic system of Au (or Cu).<sup>19</sup> The localized spin is coupled with the  $s$ -electron of the host metal which itself interacts with the other conduction electrons via what is called the Ruderman-Kittel-Kasuya-Yoshida (RKKY) Hamiltonian, thereby setting up an indirect exchange interaction between the localized moments. Because the coupling constant of the exchange interaction, in view of the RKKY coupling, alternates in sign (between ferro- and antiferromagnetic bonds), the system is “frustrated.” Thus the ground state is highly degenerate yielding a zero-temperature entropy. An additional effect is due to disorder. Because the dilute magnetic moments are quenched in at random sites, the exchange coupling strengths are randomly distributed. The dual occurrence of frustration and disorder has led to different concepts in the statistical mechanics of spin glasses such as configuration averaging, replica techniques (for computing the free energy), broken ergodicity, etc.<sup>20</sup> Experimentally, spin glasses are characterized by a “cusp” in the susceptibility and stretched exponential relaxation of time-dependent correlation functions.<sup>19</sup> It is no wonder then that spin glasses also exhibit slow dynamics with associated memory and aging effects; albeit the root causes are much more complex than a system of polydisperse, noninteracting single-domain nanomagnetic particles, discussed earlier. Indeed spin glasses, because of their complexity, have been employed as paradigms for studying real structural glasses, an unresolved problem of modern condensed matter physics.<sup>21</sup>

Given this background on two distinct physical phenomena (and yet manifestly similar properties) of superparamagnets and spin glasses, a natural question to ask is can there be spin-glass-like physics emanating from a collection of single-domain nanomagnetic particles embedded in a non-metallic, nonmagnetic host? The answer is clearly *yes* when the system is no longer a diluted one such that the supermoments start interacting via dipole-dipole coupling. Because the dipolar interaction (like the RKKY-mediated exchange interaction) is also endowed with competing ferro- and antiferromagnetic bonds,<sup>22</sup> as well as randomness due to random locations of the magnetic particles, all the attributes of spin glasses can be simulated in interacting single-domain particles. This will be analyzed below.

With the preceding discussion the plan of the paper is as follows. In Sec. II we apply the results of a rudimentary rate theory, coupled with polydispersity of the particles, to a large body of recently published data on the slow dynamics of nanomagnets. Section III deals with a different set of experiments that necessarily requires incorporation of interactions between the nanoparticles and hence spin-glass-like physics. In the concluding section IV we summarize the distinction between the superparamagnetic and collective dynamics in nanoparticle systems.

## II. SUPERPARAMAGNETIC SLOW DYNAMICS

Recently Sun *et al.* have made a series of measurements on a permalloy ( $Ni_{81}Fe_{19}$ ) nanoparticle sample which demonstrate striking memory effects in the dc magnetization.<sup>8</sup> These involve field-cooled (FC) and zero-field-cooled (ZFC) relaxation measurements under the influence of temperature and field changes. We have also observed very similar memory effects in  $NiFe_2O_4$  magnetic particles in a  $SiO_2$  host.<sup>9</sup> More recently, Sasaki *et al.*<sup>10</sup> and Tsoi *et al.*<sup>11</sup> have reported similar results for the noninteracting (or weakly interacting) superparamagnetic system of  $\gamma$ - $Fe_2O_3$  nanoparticles and ferritin (Fe-N) nanoparticles, respectively. Further, to understand the mechanisms of the experimental approach of Sun *et al.*, Zheng *et al.*<sup>12</sup> replicated the experiments on a dilute magnetic fluid with Co particles and observed similar phenomena. In this section we present a comparison of simulated results with all the above-mentioned experimental observations on the basis of a simple two-state noninteracting model plus a log-normal distribution of particle size, developed earlier in Chakraverty *et al.*<sup>9</sup> We begin our discussion from the most basic and well known protocol, viz. the zero-field-cooled magnetization (ZFCM) and the field-cooled magnetization (FCM). The analysis is based on the time-dependent magnetization, given by the formula:

$$\bar{M}(t) = \int dV P(V)M(V,t), \quad (3)$$

where  $P(V)$  is a log-normal distribution of volume  $V$ :

$$P(V) = \frac{1}{\gamma V \sqrt{2\pi}} \exp\left[-\ln \frac{V^2}{2\gamma^2}\right], \quad (4)$$

with  $\gamma$  being a fitting parameter. The rate theory expression for  $M(V,t)$  is

$$M(V,t) = M(V,t=0)\exp(-\bar{\lambda}t) + \mu VN \frac{\Delta\lambda}{\bar{\lambda}} [1 - \exp(-\bar{\lambda}t)], \quad (5)$$

where

$$\bar{\lambda} = \lambda_{0 \rightarrow \pi} + \lambda_{\pi \rightarrow 0}, \quad \Delta\lambda = \lambda_{0 \rightarrow \pi} - \lambda_{\pi \rightarrow 0}. \quad (6)$$

The parameter  $\lambda_{0 \rightarrow \pi}$  is the rate of reorientation of the magnetic moment from an angle 0 to  $\pi$ , that are directions parallel and antiparallel to the anisotropy axis, along which the magnetic field  $h$  is also applied,

$$\lambda_{0 \rightarrow \pi} = \lambda_0 \exp\left[-\frac{KV}{k_B T} \left(1 + \frac{hM_s}{2K}\right)^2\right] \left(1 + \frac{hM_s}{2K}\right), \quad (7)$$

and  $\lambda_{\pi \rightarrow 0}$  is obtained by switching the sign of  $h$ . Here  $M_s$  is the saturation magnetization per unit volume. Note that Eq. (7) is a generalization of Eq. (1) in order to take cognizance of an external field  $h$ , assuming  $h$  to be small.<sup>23,24</sup>

In the experimental procedure the external field has been taken to vary between 50 Oe to 100 Oe. The cooling or heating rate is about 2K/min. The temperature varies between 300 and 4 K. In all the simulations, the results of which are presented below, we have used a log-normal distribution of

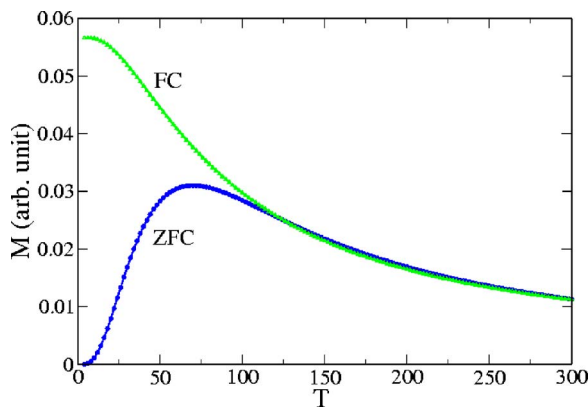


FIG. 1. (Color online) Numerically calculated dc magnetization for the FC and ZFC processes.

particle sizes wherein the parameter  $\gamma$  is set to 0.5. The average anisotropy energy  $K\bar{V}$  is chosen as the unit of energy as well as that of temperature by setting  $k_B=1$  and  $\bar{V}=\exp(\gamma^2/2)$ . The volume  $V$  is measured in units of the average volume  $\bar{V}$  and the magnetic field in units of  $K\bar{V}/M_s$ . The heating or cooling rate is set to  $r=2.4 \times 10^{12}\tau_0$  per temperature unit. Because  $\tau_0$  for nanoparticles is around  $10^{-9}$  sec and a typical experimental time window is about 10 sec, we have investigated the predictions of our model in the time window  $10^{10}\tau_0$ . After doing the simulation we reexpress the temperature and time data in K and sec for the purpose of plotting.

In all the previous studies, Sasaki *et al.*,<sup>10</sup> Tsoi *et al.*,<sup>11</sup> and Zheng *et al.*<sup>12</sup> have numerically reproduced only the ZFC and FC relaxation measurements of Sun *et al.* with temporary cooling. But in this paper we have successfully reproduced all other relaxation measurements of Sun *et al.*<sup>8</sup> based on our simple two state model. Figure 1 shows the simulated FC-ZFC curves that match well with the experimental results of Sun *et al.*<sup>8</sup> (Fig. 1). The ZFCM has a peak at  $T_{\max}=72$  K, which corresponds to the blocking temperature  $T_b$ . The magnetization of the FC curve continues to increase with decreasing temperature as would be expected for a system in thermal equilibrium. The two curves depart from one another at a temperature higher than  $T_{\max}$ . Figure 2 shows the  $M$ - $H$  curve below and above the blocking temperature  $T_b$ , indicating hysteresis below  $T_b$ .

The most striking experimental observation of Sun *et al.* is the memory effect in the dc magnetization obtained from the following procedure. The sample is cooled in 50 Oe field

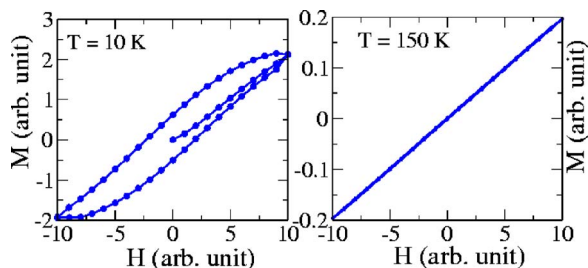


FIG. 2. (Color online) Numerically calculated  $M$  versus  $H$  curve below and above  $T_b$ .

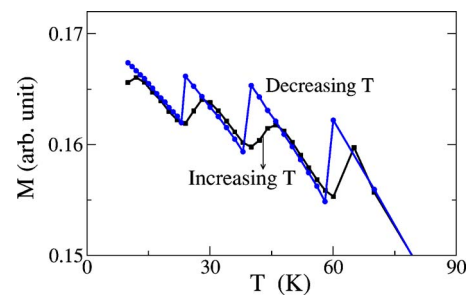


FIG. 3. (Color online) Numerically simulated memory effect observed in dc magnetization curves.

at a constant cooling rate of 2K/min from 200 K ( $T_H$ ) to 10 K ( $T_{\text{base}}$ ). After reaching  $T_{\text{base}}$ , the sample is heated continuously at the same rate to  $T_H$ . The obtained  $M(T)$  curve is the normal FC curve which is referred to as the reference curve. Then the sample is cooled again at the same rate, but the cooling is arrested three times (at  $T=70, 50,$  and  $30$  K) below  $T_b$  with a wait of  $t_w=4h$  at each stop. During  $t_w$ , the applied field is also turned off to let the magnetization decay. After each stop and wait period, the 50 Oe field is reapplied and cooling is resumed. The cooling procedure produces a steplike  $M(T)$  curve. After reaching the base temperature, the sample is warmed continuously at the same rate to  $T_H$  in the continual presence of the 50 Oe field. Surprisingly, the  $M(T)$  curve obtained in this way also shows the steplike behavior. Similar memory effects, following the same protocol, were seen by us in the  $\text{NiFe}_2\text{O}_4$  sample in which the magnetic particles were embedded in a host  $\text{SiO}_2$  matrix.<sup>9</sup> Although the effects were earlier explained in terms of a bimodal distribution of particle size,<sup>9</sup> a log normal distribution in the simulation also indicates satisfactory agreement with experiments, as seen in Fig. 3.

In the Sun *et al.* measurements<sup>8</sup> for magnetic relaxation with temporary cooling and field change for the ZFC method the sample is cooled to  $T_0=30$  K in zero field. Then a 50 Oe field is applied and the magnetization is measured for a time  $t_1$ . After  $t_1$ , the sample is quenched to temperature  $T=22$  K in the absence of an external field and the magnetization is recorded for a time  $t_2$ . Finally the temperature is returned back to  $T_0$  and the field is turned on again. The magnetization is measured for a time  $t_3$ .

In Fig. 4 we show our corresponding numerically simulated results. When a field of 50 Oe is applied the magnetization immediately reaches a certain value, because the particles with  $T_b \leq 30$  K equilibrate rapidly. Then a slow logarithmic response begins which is due to the energy distribution of the particles.<sup>25</sup> Now as the field is turned off, we observe a sharp jump in  $M(t)$  due to those particles with  $T_b \leq 22$  K which reach their equilibrium state at  $T=22$  K and hence do not contribute to the magnetization. However, the particles with  $T_b > 30$  K are not in equilibrium and relax extremely slow at  $T=22$  K, so we get a constant curve during  $t_2$ . Now as the field is turned on again and the temperature of the sample is increased to  $T=30$  K, the particles with  $T_b \leq 30$  K and those flipped during time  $t_1+t_2$  come back to the new equilibrium state which is same as that pertaining before quenching. Therefore, the relaxation in  $t_3$  is the continuation of that during the time  $t_1$ .

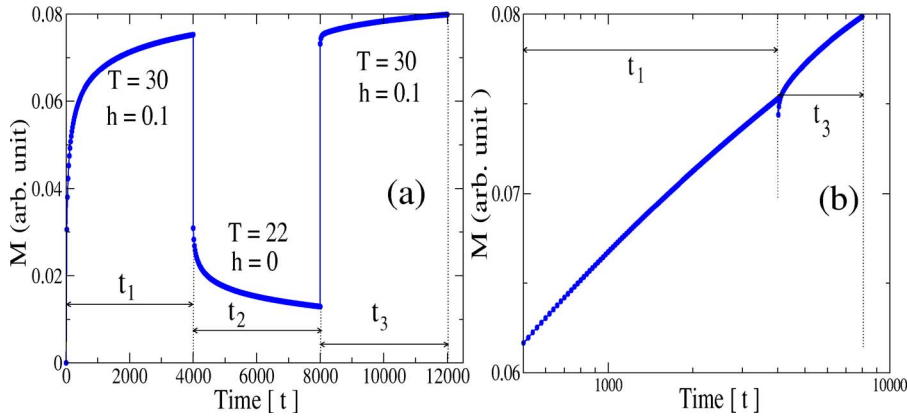


FIG. 4. (Color online) (a) Numerically simulated ZFC relaxation curves with temporary cooling and field change; (b) the same data vs the total time spent at 30 K on a logarithmic scale.

In the FC magnetic relaxation with temporary cooling and field change the sample is cooled to  $T_0=30$  K in a 50 Oe field and then the relaxation is measured for a time  $t_1$  after the field is cut off. The field is turned on again and the sample is cooled to  $T=22$  K and the magnetization is recorded for a time  $t_2$ . Finally the temperature is turned back to  $T_0$  and the field is switched off again. The relaxation is now measured for a time  $t_3$ .

We represent our numerical results for the same protocol in Fig. 5. When the field is cut off the particles with  $T_b \leq 30$  K do not contribute to the magnetization. After  $t_1$ , when the sample is quenched to 22 K and the field is turned on, there is naturally a sudden jump in the magnetization due to the particles with  $T_b \leq 22$  K which have much higher magnetization than the value just before quenching. As discussed earlier the particles with  $T_b > 30$  K are not in equilibrium and their relaxation is very slow at  $T=22$  K, which explains an almost constant curve during  $t_2$ . After  $t_2$ , the field is turned off, and the temperature is turned back to  $T_0$ . Naturally, the magnetization jumps down, because the particles with  $T_b \leq 30$  K reach a new equilibrium state which has almost zero magnetization immediately following the field and temperature changes and the system returns back to its state prevailing before quenching.

Finally, Sun *et al.* have studied magnetic relaxation after a temporary heating (instead of temporary cooling) from 30 to 38 K which does not exhibit any memory effect. After temporary heating, when the temperature returns to  $T_0$ , the system does not come back to its previous state before heating. Sun *et al.* suggested that this asymmetric response with respect to negative/positive temperature cycling is consistent

with a hierarchical model of the spin-glass phase. However, we have numerically reproduced the same results as that of Sun *et al.* based on our two-state independent particle model, as shown in Fig. 6. No memory effect appears after positive heating which can be explained as follows. In the FC method the sample is cooled to  $T_0=30$  K in the presence of a 50 Oe field and then the field is cut off and the relaxation is measured for a time  $t_1$ . So the magnetization decreases with time for a time  $t_1$ . Now as the temperature is increased all the particles with  $T_b \leq 38$  K respond to this temperature change and relax to the new equilibrium state. Since thermal agitation increases with the increase of temperature, the magnetization decreases further for the time  $t_2$ . As the temperature returns back to  $T=30$  K, the particles with  $T_b > 30$  K are unable to respond to this temperature change. Thus the particles with  $T_b \leq 30$  K actually follow the path during time  $t_2$  rather than  $t_1$ . Because all the particles which had flipped during the time  $t_1+t_2$  cannot return back to their previous state as that before heating, no memory effect is observed.

In the ZFC method the sample is cooled to  $T_0$  in the absence of an external field and then a 50 Oe field is turned on and relaxation is measured for a time  $t_1$ , yielding a finite magnetization, for particles with  $T_b \leq 30$  K. Then a slow logarithmic relaxation begins which is due to the energy distribution of the particles. As the sample is further heated to  $T=38$  K, all the particles with  $T_b=38$  K respond to this temperature change. Thus the logarithmic relaxation is continued but there is a jump in magnetization, because the particles with  $T_b \leq 38$  K and those flipped during  $t_1$  reach a new equilibrium state. As the temperature of the sample is returned back to  $T=30$  K thermal agitation is reduced, so there is a

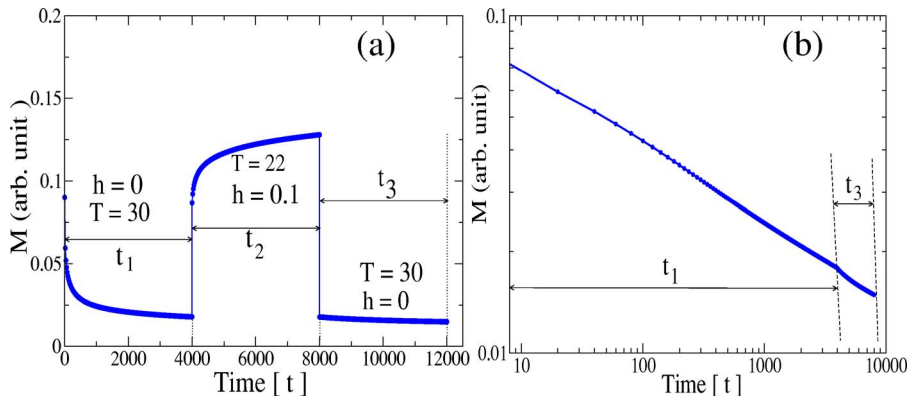


FIG. 5. (Color online) (a) Numerically simulated FC relaxation curves with temporary cooling and field change; (b) the same data vs the total time spent at 30 K on a logarithmic scale.

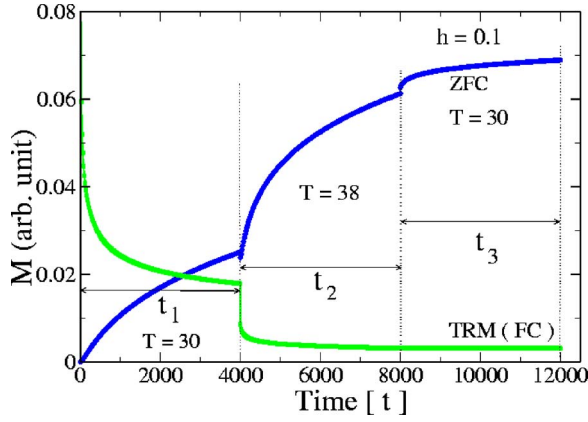


FIG. 6. (Color online) Numerically simulated FC and ZFC relaxation curves with temporary heating.

jump in magnetization. But now only the particles with  $T_b > 30$  K are allowed to relax and their relaxation is very slow at  $T=30$  K, so we obtain an almost flat curve.

We conclude this section by underscoring that our simulations based on the simple two-state noninteracting model reproduce all the features of the memory effects observed by Sun *et al.* in the Permalloy ( $\text{Ni}_{81}\text{Fe}_{19}$ ). Secondly, positive heating does not yield memory effect whereas temporary cooling does. So there is an asymmetric response with respect to negative/positive temperature cycling. This asymmetry is due to the fact that after temporary cooling only smaller nanoparticles are able to respond to the temperature or field change and relax to the new equilibrium state. The larger nanoparticles are frozen. Upon returning to the initial temperature or field value, the smaller particles rapidly respond to the change such that this new state is essentially the same as that before the temporary cooling, and the larger nanoparticles are now able to resume relaxing to the equilibrium state. This results in a continuation of the magnetic relaxation after the temporary temperature or field change. In contrast, for positive heating, all the particles, smaller as well as bigger, are able to respond to the temperature or field change. Therefore, after returning to the initial temperature, the bigger particles do not respond at all whereas the smaller particles take time to respond, thus leading to no memory effect in the positive heating cycle.

### III. SPIN-GLASS-LIKE SLOW DYNAMICS

Time-dependent magnetization measurements suggest that dense nanoparticle samples may exhibit glassy dynamics due to dipolar interparticle interaction,<sup>16,26–28</sup> disorder and frustration are induced by the randomness in the particle positions and anisotropy axis distributions. As discussed within a simple mean field theory picture, adapted to the two-state model of Chakraverty *et al.*,<sup>9</sup> the random dipolar interaction can be accounted for in terms of a local, self-consistent field that has the form

$$\mathcal{H} = \mu V \Lambda \tanh\left(\frac{\mu V \mathcal{H}}{k_B T}\right), \quad (8)$$

$\Lambda$  being a random variable. As Eq. (8) admits both positive and negative solutions for  $\mathcal{H}$ , corresponding to ferro- and antiferromagnetic bonds, frustration is automatically incorporated within the simplified two-state picture. The rate constant in Eq. (7) is thus modified replacing  $h$  by  $h + \mathcal{H}$ .

The ZFC and FC behavior (for the magnetization) for the dense magnetic nanoparticle system, as measured by Sasaki *et al.*,<sup>10</sup> is numerically simulated by us and shown in Fig. 7. We observe a peak in the ZFCM which corresponds to an average blocking temperature  $\langle T_b \rangle$ . In the superparamagnetic case the ZFC-FC curves bifurcate at a temperature away from the peak position of the ZFCM (see Fig. 1). On the other hand, for the dense system the ZFCM-FCM curves bifurcate at a temperature very close to the peak position of the ZFCM. The FCM of the dense system does not increase but stays almost constant below  $\langle T_b \rangle$  which is the primary indicator for the glassy state.<sup>10</sup>

In order to have a better understanding of glassy relaxation, time-dependent magnetization studies under various heating and cooling protocols were performed by Sasaki *et al.*<sup>10</sup> on dense Fe-N nanoparticle systems, by Sankar *et al.*<sup>14</sup> on  $\text{LaMnO}_{3,13}$ , by Kundu *et al.* on  $\text{La}_{07}\text{Ca}_{0.3}\text{CoO}_3$  (Ref. 15), and by Telem-Shafir and Markovich on the MICS76 sample.<sup>16</sup> In a double memory experiment (DME) under FC protocol the system is cooled under a field of 50 Oe. The field is cut off during the intermittent stops of the cooling at  $T=30$  K and at  $T=40$  K for 3000 sec at each stop. After reaching the lowest temperature the magnetization measurement is repeated in the heating mode without any intermit-

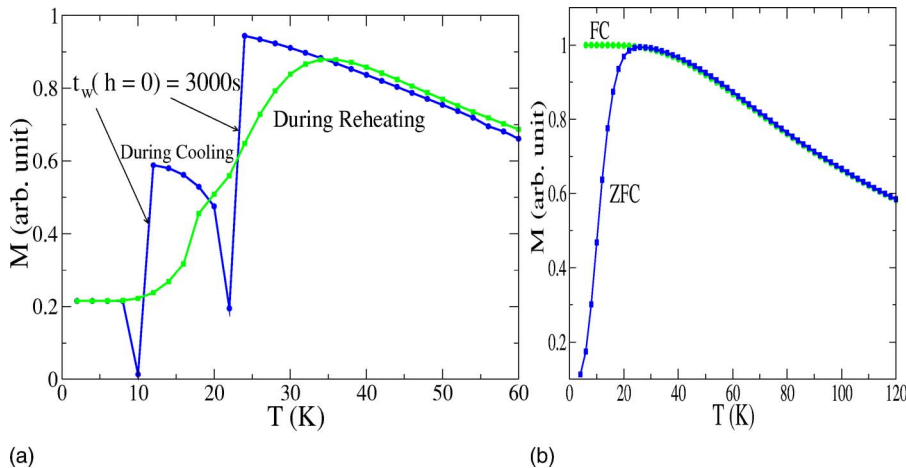


FIG. 7. (Color online) (a) Numerically simulated results for the double memory experiment (DME) for the FC method; (b) the FCM and ZFCM vs temperature of the interacting system are shown.

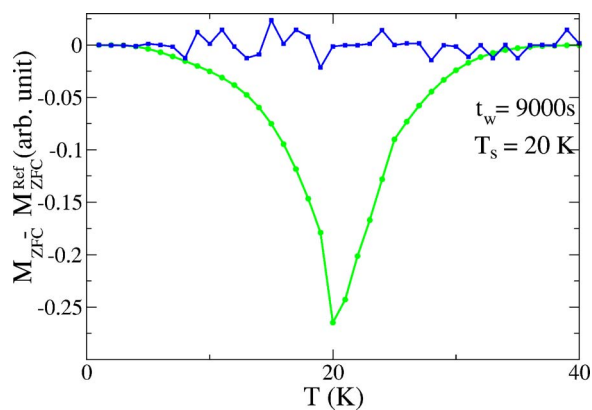


FIG. 8. (Color online) Numerically simulated results for the double memory experiment (DME) for the ZFC method in an interacting system (green circle) and in a noninteracting system (blue square).

tent stop. In Fig. 7(a) we have shown our numerically simulated results of DME based on our interacting nanoparticle model, which have a striking resemblance to the experimental results.

Another protocol has been suggested by Sasaki *et al.* to confirm whether the observed memory effect is due to glassy behavior or not. In this, the sample is first rapidly cooled in zero field from a reference temperature ( $T_{\text{ref}}$ ) to the stop temperature ( $T_s$ ), where it is kept for 9000 sec. The cooling is then resumed down to the lowest temperature where a magnetic field is applied and the susceptibility is recorded on reheating the sample. The conventional ZFC susceptibility is also recorded. The difference between the aged and the normal ZFC susceptibility as a function of temperature was measured by Sasaki *et al.*<sup>10</sup> Figure 8 is our numerically simulated results, which are again very similar to that of the experiment. In the fitting procedure Eq. (8) has been numerically solved by choosing  $\Lambda$  randomly between 0 and 1, fixing  $h$  to 0.5, as before.

#### IV. SUPERPARAMAGNETISM VERSUS SPIN-GLASS

From the above analysis it is evident that the slow dynamics in nanoparticle systems can be classified into two kinds. The first one is due to the broad distribution of relaxation times originating solely from the anisotropy energy barriers. In this noninteracting case the magnetic moment of each particle relaxes according to its individual energy barrier, that depends on the magnetic anisotropy, which in turn depends on the volume of the nanoparticle. Therefore, a distribution of particle volumes results in a distribution of energy barriers and blocking temperatures. In the second kind of slow dynamics in dense magnetic nanoparticle systems, cooperative spin-glass-like dynamics, accompanied by frustration caused by the strong dipolar interactions among the particles, are the underlying reasons for memory effects. Here no unique ground state exists but rather many configurations are equally probable. The local energy barriers between these configurations are low, enabling a constant development towards equilibrium, but resulting in the inability to reach it.

Which kind of slow dynamics amongst the two scenarios, presented above, is relevant depends essentially on the concentration of the nanoparticles, at least for the data shown here. One indicator of the difference in the two kinds of slow dynamics of noninteracting and interacting nanoparticles is revealed by the field-cooled (FC) magnetization measurements. The extent of the memory effect can be quantified by a parameter ( $R$ ) (Ref. 9)

$$R = \Theta \left( \frac{dM}{dT} \right)_{T=T_n} \frac{dM}{dT}, \quad (9)$$

where  $\Theta(x)$  is the Heaviside step function and  $T_n$  is the temperature at which field is switched off. This parameter measures the positive slope of the  $M(T)$  curve during zero field heating. We have calculated  $R$  for the noninteracting and interacting cases from Fig. 3 and 7(a), respectively. The value of  $R$  in the dense system is about eight times larger than that in the noninteracting case, implying that the magnitude of the FC magnetization memory effect does depend on the interparticle dipolar interaction. This is in quite good agreement with the experimental results of Telem-Shafir *et al.*<sup>16</sup>

In the noninteracting case, no memory effect is seen during a ZFC process (see Fig. 8) below ( $T_b$ ), since the occupation probabilities of up and down particles are both equal to 0.5 (two-state model). So this system does not show any difference between the magnetization curves with and without intermittent stops during the cooling process. But in the interacting case there exists a huge number of states, because the local mean dipolar field is a random variable. The system goes into deeper and deeper valleys with higher and higher energy barriers as time progresses. Therefore, the energy barrier of the state in which the system is blocked depends on the aging time of the system, when temperature is low, and the consequent higher energy barrier makes the system more reluctant to respond to an applied field. Thus the difference in the energy barrier with and without intermittent stops on cooling causes the dip in Fig. 8. Further the memory effect observed in the ZFC method in the interacting case can be observed over a temperature range, albeit narrow, below  $T_b$ . It can therefore be said that although no true superparamagnetic to spin-glass phase transition occurs in the strongly interacting case, a sharp transition from a superparamagnetic state towards local domains of stable magnetic moments does occur very close to  $T_b$ .

The third significant difference between “superspin” and “superparamagnet” is in the behavior of the FCM. The latter for the superparamagnet increases with the decrease of temperature whereas it not only does not increase but can even decrease as the temperature is lowered for the interacting sample (see Figs. 1 and 7). The individual blocking model reproduces a monotonous increase in FCM for “superparamagnets.” The field-cooled magnetization increases with decreasing temperature until all particles are blocked. Such features reflect a distribution of  $T_b$ , i.e., distribution of particle volumes. On the other hand, the temperature independence of the FCM for the “superspines” cannot be explained by the

individual particle model and is a clear indication of progressive freezing of particle moments which behave in a collective manner.

## V. CONCLUSIONS

In conclusion, similarities as well as distinct differences in the slow dynamics of isolated nanoparticles and of strongly interacting nanoparticles are discussed. Our interacting and noninteracting models are adequate to capture all these signatures. From the comparative study, it is well understood

that the similarities are observed in the memory effect following the temperature and field protocol of Sun *et al.* On the other hand, the differences are seen in the FC memory effect, ZFC memory effect, and in the FCM.

## ACKNOWLEDGMENTS

M.B. acknowledges financial support from the Council of Scientific and Industrial Research (CSIR), Government of India. S.D. is grateful to G. Markovich and C. N. R. Rao for helpful discussions on their experimental results during an Indo-Israeli symposium on nanosciences in Bangalore.

---

\*Present address: Indian Institute of Science Education and Research, HC-VII, Salt Lake, Kolkata 700106, India.

- <sup>1</sup>L. Neel, *Ann. Geophys. (C.N.R.S.)* **5**, 99 (1949).
- <sup>2</sup>J. Frankel and J. Dorfman, *Nature (London)* **126**, 274 (1930); C. Kittel, *Phys. Rev.* **70**, 965 (1946).
- <sup>3</sup>C. P. Bean and J. D. Livingstone, *J. Appl. Phys.* **30**, 120S (1259); I. S. Jacobs and C. P. Bean, in *Magnetism*, edited by G. T. Rado and H. Suhl (Academic, New York, 1963), Vol. 3.
- <sup>4</sup>E. P. Wohlfarth, *J. Phys. F: Met. Phys.* **10**, L241 (1980).
- <sup>5</sup>W. F. Brown, Jr., *Phys. Rev.* **130**, 1677 (1963).
- <sup>6</sup>J. P. Bouchaud, L. Cugliandolo, J. Kurchan, and M. Mezard, in *Spin Glasses and Random Fields*, edited by A. P. Young (World Scientific, Singapore, 1998).
- <sup>7</sup>M. Mezard, G. Parisi, N. Sourlas, G. Toulouse, and M. Virasoro, *Phys. Rev. Lett.* **52**, 1156 (1984).
- <sup>8</sup>Y. Sun, M. B. Salamon, K. Garnier and R. S. Averbach, *Phys. Rev. Lett.* **91**, 167206 (2003); M. Sasaki, P. E. Jönsson, H. Takayama, and P. Nordblad, *Phys. Rev. Lett.* **93**, 139701 (2004); R. K. Zheng, H. Gu, and X. X. Zhang, *Phys. Rev. Lett.* **93**, 139702 (2004); Y. Sun, M. B. Salamon, K. Garnier, and R. S. Averbach, *Phys. Rev. Lett.* **93**, 139703 (2004).
- <sup>9</sup>S. Chakraverty, M. Bandyopadhyay, S. Chatterjee, S. Dattagupta, A. Frydman, S. Sengupta, and P. A. Sreeram, *Phys. Rev. B* **71**, 054401 (2005).
- <sup>10</sup>M. Sasaki, P. E. Jönsson, H. Takayama, and H. Mamiya, *Phys. Rev. B* **71**, 104405 (2005).
- <sup>11</sup>G. M. Tsoi, L. E. Wenger, U. Senaratne, R. J. Tackett, E. C. Buc, R. Naik, P. P. Vaishnava, and V. Naik, *Phys. Rev. B* **72**, 014445 (2005).
- <sup>12</sup>R. K. Zheng, Hongwei Gu, Bing Xu, and X. X. Zhang, *Phys. Rev. B* **72**, 014416 (2005).
- <sup>13</sup>X. Chen, S. Bedanta, O. Petracic, W. Kleemann, S. Sahoo, S. Cardoso, and P. P. Freitas, *Phys. Rev. B* **72**, 214436 (2005).
- <sup>14</sup>C. R. Sankar and P. A. Joy, *Phys. Rev. B* **72**, 132407 (2005).
- <sup>15</sup>A. K. Kundu, P. Nordblad, and C. N. R. Rao, *Phys. Rev. B* **72**, 144423 (2005).
- <sup>16</sup>T. Telem-Shafir and Gil Markovich, (unpublished).
- <sup>17</sup>R. Street and J. C. Wooley, *Proc. Phys. Soc., London, Sect. A* **62**, 562 (1949).
- <sup>18</sup>S. Dattagupta, *Relaxation Phenomena in Condensed Matter Physics* (Academic, Orlando, 1987).
- <sup>19</sup>J. A. Mydosh, *Spin Glasses, An Experimental Introduction* (Taylor & Francis, London, 1993).
- <sup>20</sup>M. Mezard, G. Parisi, and M. A. Virasoro, *Spinglass Theory and Beyond* (World Scientific, Singapore, 1987).
- <sup>21</sup>C. Dasgupta, *Pramana* **64**, 679 (2005); in *Proceedings of the 22nd International Conference on Statistical Physics*, edited by S. Dattagupta, H. R. Krishnamurthy, R. Pandit, T. V. Ramakrishnan, and D. Sen (Indian Academy of Sciences, Bangalore, 2005).
- <sup>22</sup>J. M. Luttinger and L. Tisza, *Phys. Rev.* **70**, 954 (1946).
- <sup>23</sup>Amikam Aharoni, *Phys. Rev.* **177**, 793 (1969).
- <sup>24</sup>E. Kneller and E. P. Wohlfarth, *J. Appl. Phys.* **37**, 4816 (1966).
- <sup>25</sup>J. Tejada, X. X. Zhang, and E. M. Chudnovsky, *Phys. Rev. B* **47**, 14977 (1993).
- <sup>26</sup>W. Luo, S. R. Nagel, T. F. Rosenbaum, and R. E. Rosensweig, *Phys. Rev. Lett.* **67**, 2721 (1991).
- <sup>27</sup>H. Mamiya, I. Nakatani, and T. Furubayashi, *Phys. Rev. Lett.* **82**, 4332 (1999).
- <sup>28</sup>P. Jönsson, M. F. Hansen, and P. Nordblad, *Phys. Rev. B* **61**, 1261 (2000).